Magma-assisted rifting in Ethiopia

Magma-assisted rifting in Ethiopia

J.-M. Kendall[1], G. W. Stuart[1], C. J. Ebinger[2], I. D. Bastow[1] & D. Keir[2]

[1]School of Earth Sciences, University of Leeds, Leeds LS2 9JT, UK
[2]Department of Geology, Royal Holloway, University of London, Egham, Surrey TW20 0EX, UK

The rifting of continents and evolution of ocean basins is a fundamental component of plate tectonics, yet the process of continental break-up remains controversial. Plate driving forces have been estimated to be as much as an order of magnitude smaller than those required to rupture thick continental lithosphere[1,2]. However, Buck[1] has proposed that lithospheric heating by mantle upwelling and related magma production could promote lithospheric rupture at much lower stresses. Such models of mechanical versus magma-assisted extension can be tested, because they predict different temporal and spatial patterns of crustal and upper-mantle structure. Changes in plate deformation produce strain-enhanced crystal alignment and increased melt production within the upper mantle, both of which can cause seismic anisotropy[3]. The Northern Ethiopian Rift is an ideal place to test break-up models because it formed in cratonic lithosphere with minor far-field plate stresses[4,5]. Here we present evidence of seismic anisotropy in the upper mantle of this rift zone using observations of shear-wave splitting. Our observations, together with recent geological data, indicate a strong component of melt-induced anisotropy with only minor crustal stretching, supporting the magma-assisted rifting model in this area of initially cold, thick continental lithosphere.

The data we analysed were collected as part of the EAGLE project (Ethiopian Afar Geophysical Lithospheric Experiment), an international multi-institutional experiment designed to investigate rifting processes in Ethiopia[6]. The Miocene–Recent Ethiopian Rift (Fig. 1) constitutes the northern part of the East African Rift system and forms one arm of a triple junction that formed on or near a mantle plume. Our study region is transitional between continental and incipient oceanic, with strain localized to <20-km-wide zones of dyking, faulting and volcanism[6,7]. It is an ideal place to study magmatism and plate rupture, because up to 25% of the crust is extruded lava or intrusive magma[7,8] and mantle lithosphere is thin (<50 km) beneath the rift valley[9].

Seismic data were acquired in three phases of the EAGLE project[6], two of which were designed to record passive seismicity. In phase I, 29 broad-band seismometers were deployed for 16 months with a nominal station spacing of 40 km and covering a 250 km × 350 km region centred on the transitional part of the rift (Fig. 1). In phase II, a further 50 instruments were deployed for three months in a tighter array (nominal station spacing of 10 km) in the rift valley. Our study of mantle anisotropy is based on evidence of shear-wave splitting in the teleseismic phases SKS, SKKS and PKS recorded by these two arrays. With the longer duration array, 15 events produced usable splitting results, and with the shorter duration rift-valley array, three events produced usable results (list of events given in Supplementary Information).

Shear-wave splitting analysis of the seismic phases SKS, SKKS and PKS is now a standard tool for studying upper-mantle anisotropy[10,11]. SKS, for example, propagates as an S-wave through the mantle and a P-wave through the Earth's core. As such, in an isotropic radially stratified Earth, SKS should exhibit linear particle motion and be visible only on the radial and vertical components of a seismometer. However, this phase will be split into a fast and slow shear-wave should it cross an anisotropic region on the receiver side of its path through the mantle. This will produce an elliptical particle motion and energy on the transverse component. The splitting can be quantified by the time delay between the two shear waves (δt) and the orientation of the fast shear wave (ϕ). To remove the effects of the anisotropy one can rotate the horizontal components by ϕ and shift their relative positions by δt, thereby linearizing the particle motion and removing the transverse component energy on the seismograms[10,11]. To estimate the splitting we search for the correction parameters that best linearize the SKS motion (that is, minimize the smaller eigenvalue of the covariance matrix). A statistical *F*-test is used to assess the uniqueness of the estimated splitting parameters and thereby provides an error estimate[10].

The SKS splitting results obtained from the Ethiopian data are of exceptional quality and resolution (see Supplementary Information for some examples and list of results). We have obtained a remarkable 327 SKS splitting observations in a region focused on the Northern Ethiopian Rift. The anisotropy parameters are well constrained and we use a cutoff error criteria of ±0.6 s for δt and 10° for ϕ. In general, the orientation of the fast shear wave is roughly parallel to the trend of the rift and the magnitude of the splitting varies from 1.0 to 3.0 s (Figs 1, 2). The larger delay times are some of the largest SKS-splitting results ever reported (see ref. 10). The generally rift-parallel alignment is in agreement with other SKS[12–15] and surface-wave[16] studies of anisotropy along the East African Rift and in Afar. A detailed study of SKS splitting at the permanent Ethiopian IRIS station FURI reveals little dependence on incoming back-azimut (direction from station to earthquake), thus suggesting a uniform layer of anisotropy with a horizontal symmetry axis[13]. Furthermore, the magnitude of the splitting can vary considerably

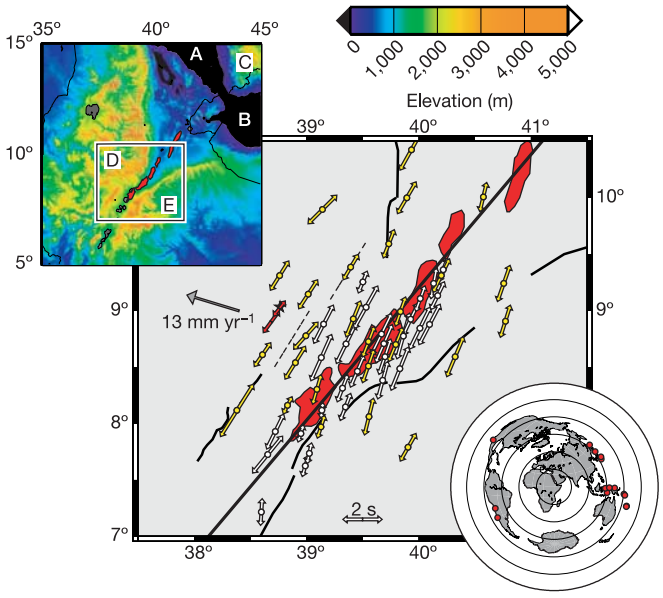

Figure 1 SKS splitting results in the region of the Northern Ethiopian Rift. The orientation of arrows shows the alignment of fast shear waves and the length of the arrow is proportional to the magnitude of the splitting. Yellow arrows mark results at seismic stations deployed for 16 months, white arrows are for stations deployed for three months, and red arrows are for the IRIS permanent stations FURI and AAE. In total, the results represent >350 splitting measurements. Heavy black lines show major border faults, dashed lines show monoclines and magmatic segments are marked in red. The solid black line bisecting the magmatic segments shows the approximate rift axis used to construct Fig. 2c and d. The top left inset shows the topography and magnetic segments in the region of interest (A, Red Sea; B, Gulf of Aden; C, Arabian plate; D, Nubian plate; E, Somalian plate). The lower right inset shows the locations of events used for shear-wave splitting analysis. Concentric circles mark 30° increments in distance from the array.

over a short distance (50 km). Arguments based on the wavelength of SKS phases therefore constrain the differences in anisotropy to the upper 100 km (ref. 17). However, we cannot preclude the possibility of an additional contribution from a deeper uniform layer of anisotropy.

Closer inspection of the results reveals systematic variations in the splitting parameters (Fig. 2). The orientation of the fast shear wave (ϕ) shows a well resolved rotation counter-clockwise within the rift valley. Figure 2a shows that ϕ varies from 40° on the NW–SE flanking plateaus on the Nubia and Somalia plates to 15° within the rift valley. The variation in the magnitude of splitting also varies across the rift. The highest splitting values are observed at the edges of the fault-bounded rift valley; this is especially apparent on the SE side of the rift valley (Fig. 2b). The orientation of the anisotropy within the rift valley is constant from SW to NE (Fig. 2c). In the SW (continental region), the magnitude of splitting is roughly 1 s, whereas in the NW (more oceanic region) the splitting is >1.6 s (Fig. 2d). These results agree with splitting parameters from the permanent stations KMBO in Kenya and ATD in Djibouti, respectively[13,18]. The highest splitting occurs in the region where the rift valley orientation changes from NNE to NE before broadening into the Afar depression. This ENE-trending, $<$11-million-year (Myr) sector of the Ethiopian Rift effectively links the originally discrete East African Rift to the Oligocene southern Red Sea Rift[19].

Such anisotropy could be due to the preferential alignment of minerals, or the preferential vertical alignment of inclusions such as crack-like melt inclusions, or some combination of these mechanisms. A range of plausible processes could lead to such anisotropy, including pre-existing anisotropy frozen into the surrounding lithosphere, anisotropy due to asthenospheric flow in the direction of absolute plate motion (APM), and anisotropy associated with rifting processes. Most of these, however, can be eliminated. Shear zones and metamorphic fabric within Precambrian basement rocks, where they are exposed, strike N–S, and Mesozoic rift structures strike NW[20,21]. Thus, pre-existing deformation fabric cannot explain the strong NE alignment we observe. Furthermore, Africa is nearly stationary (6 mm yr^{-1}) (ref. 4) in an absolute hotspot reference frame[5], and the anisotropy is roughly orthogonal to the APM direction, thus ruling out anisotropy due to the motion of the African plate over the mantle.

Instead, the anisotropy is most probably caused by rifting processes. Simple two-dimensional tectonic extension would lead to the alignment of olivine in the direction of extension or spreading direction[22,23], as has been observed at the East Pacific Rise[24]. In contrast, our data show rift-parallel fast directions (ϕ) that are perpendicular to tectonic extension. The rift-parallel anisotropy could be caused by channelled horizontal mantle flow along the rift[23], or the preferred alignment of melt-filled cracks, or dykes emanating from the upper mantle and aligned parallel to rifting[12–14,25]. We consider both models in the light of independent data. If we assume a 60° dip of the lithosphere–asthenosphere boundary beneath the rift and the ratio of pre-rift to present lithospheric thickness of $\beta = 1.5$ (ref. 19), then the zone of mantle lithospheric stretching would be 60 km wider than the 80-km-wide rift at the surface. Hence, rift effects could influence the entire region beneath our array. The differences in channelled flow would have to be quite shallow, owing to the rapid change in splitting parameters, and then either the thickness of the flow layer would increase moving north-eastward towards Afar, or the degree of strain, and hence crystal alignment, would increase in this direction. The orientation of the anisotropy mimics the distribution of Quaternary strain and magmatism (magmatic segments, Fig. 1). Structural, geochemical and seismic data indicate that magmatic segments are zones of intense dyke injection and magmatic intrusion[6,7,19], with many dyke-fed mafic lavas sourced within the asthenosphere[26]. En

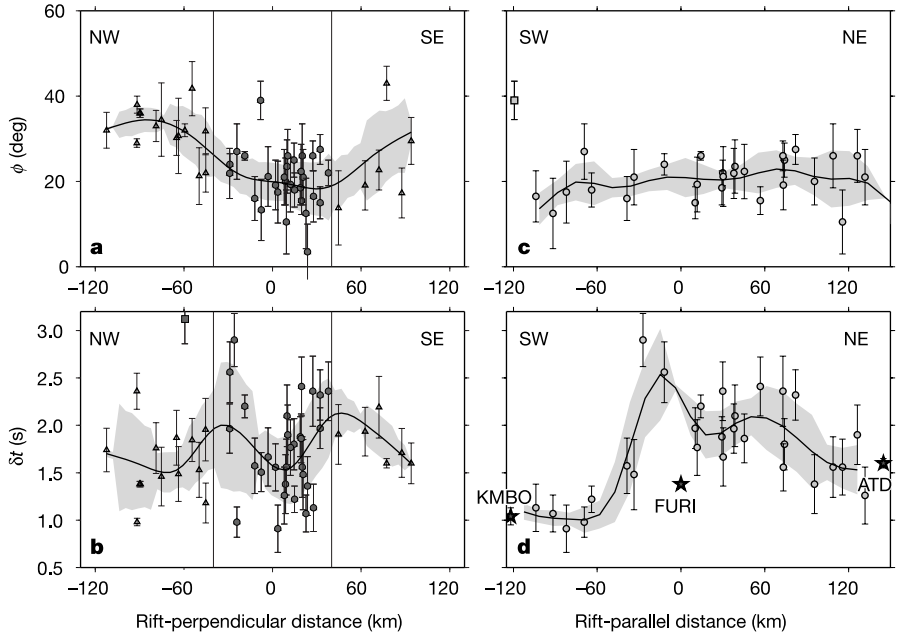

Figure 2 Shear-wave splitting parameters, ϕ (top panels) and δt (bottom panels), as a function of distance perpendicular to the rift (NW to SE) (left panels) and distance along the rift moving from the SW to the NE (right panels). The assumed axis of the rift valley is shown in Fig. 1 and the valley is assumed to be 80 km wide. In **a** and **b**, flanks of the rift are marked by vertical lines and the results for stations within the rift are marked by circles. Error bars show uncertainty in individual measurements. In each panel the solid line shows an interpolated fit to the data using a cubic B-spline interpolation with a knot spacing of 30 km. The shaded region shows the r.m.s. misfit of the data from the curve over a 30-km sliding window (squares mark outliers in **b** and **c** that are not included in the interpolation). For reference, results for permanent stations in Kenya (KMBO), Ethiopia (FURI) and Djibouti (ATD) are also indicated in **d** as star symbols. Note that KMBO and ATD are respectively well removed from the most southerly and northerly stations and that FURI is not within the rift valley.

echelon Quaternary magmatic segments are orientated NNE–SSW, oblique to the orientation of Mid-Miocene border faults bounding the rift[19], but parallel to the fast shear-wave polarizations. We note, for example, how ϕ parallels the border faults to the NW, but rotates to parallel the magmatic segments within the rift (Fig. 1). The correlation with orientations of dykes and faulted dykes within magmatic segments strongly suggests that the anisotropy is associated with magmatic processes.

It is plausible that both aligned melt intrusion zones within the lithosphere and aligned asthenospheric flow mechanisms for anisotropy are at play in this transitional rift. Recent laboratory simulations of dunite deformation show strain partitioning and melt segregation[27]. The resulting anisotropy will be due to three mechanisms: the preferred alignment of olivine; the preferred alignment of ellipsoidal melt inclusions; and the layering of melt-rich and melt-poor bands. In the case of vertically upwelling material, this model predicts the horizontal alignment of olivine crystals, with melt inclusions and melt bands aligned parallel to a sheet-like upwelling[27]. The aligned melt will be a dominant effect in high-strain regions. The alignment of less than 0.1% melt fraction in the upper 70–90 km would explain the magnitude of the splitting[13] and be consistent with observed changes in splitting over distances of the order of 50 km (ref. 17). Major-element compositions of Quaternary magmatic products erupted near the western rift margin suggest the onset of melting occurs at depths of 60–75 km (ref. 26). Strain partitioning will be greatest beneath the rift flanks, thus explaining the high magnitude of splitting at the rift margins and where the Ethiopian Rift bends into the more extended and oceanic Afar region. Also, steep gradients at the lithosphere–asthenosphere boundary, as imaged by travel-time tomography[9], would not only enhance flow velocities, but also lead to enhanced melt extraction. Melt would flow along pressure gradients before emplacement within the lithosphere[28].

Our aligned melt-filled crack model can explain the parallelism of anisotropy and the strikes of dykes and aligned eruptive centres in magmatic segments, and it provides a mechanism that can relate magnitude of anisotropy to volume of magmatism. There is increased splitting with increased magma production near break-up. The melt will solidify, moving away from the mantle upwelling, leaving a residual anisotropy predominantly due to crystal alignment. Just as dykes strike perpendicular to the local extension direction, our model's splitting directions outside and within the $<$2-Myr magmatic segments confirm the previously reported change from N130°E-directed extension to N110°E-directed extension at $\sim$2 Myr, when crustal strain localized to magmatic segments[19].

The close station distribution and large number of instruments deployed in EAGLE provide the first images of seismic anisotropy along and across a zone of incipient continental break-up. The large magnitude of splitting and the correlation of splitting with magmato-tectonic features within the rift help constrain melt production and strain partitioning, allowing us to test current models of continental break-up. Detachment–fault models of lithospheric stretching predict comparable but offset amounts of crust and mantle lithospheric thinning, with high strain zones along one side (detachment) of an asymmetric rift[29]. However, there is little support for this model in the seismic images[8,9], and such a model predicts anisotropy that produces fast shear-wave alignment perpendicular to the rift[23], not parallel to the rift, as we observe. EAGLE wide-angle data show small amounts of crustal thinning and little asymmetry[8] ($\beta \leq 1.5$), yet tomographic images indicate considerable mantle lithospheric thinning. Although detachment faults may have been active during the first $\sim$8 Myr of rifting in Ethiopia, they were abandoned as thinning and heating produced a ready supply of magma, locally weakening the plate and concentrating strain[19]. Geodetic measurements show that $\sim$80% of the strain is accommodated in magmatic segments[30], probably via intensive aseismic dyke injection[7]. Our results support magma-assisted rifting of initially thick, strong continental lithosphere[1,7], because they predict a broad region of magma injection in the mantle lithosphere beneath a relatively unstretched, but heavily intruded crust. □

Received 23 June; accepted 3 November 2004; doi:10.1038/nature03161.

1. Buck, W. R. in *Rheology and Deformation of the Lithosphere at Continental Margins* (eds Karner, G. D., Taylor, B., Driscoll, N. W. & Kohlstedt, D. L.) 1–30 (Columbia Univ. Press, New York, 2004).
2. Bott, M. H. P. Sublithospheric loading and plate-boundary forces. *Phil. Trans. R. Soc. Lond.* **337,** 83–93 (1991).
3. Kendall, J.-M. in *Earth's Deep Interior: Mineral Physics and Tomography from the Atomic to the Global Scale* (eds Karato, S., Stixrude, L., Liebermann, R. C., Masters, T. G. & Forte, A. M.) 149–175 (Geophys. Monogr. Ser. 117, American Geophysical Union, Washington DC, 2000).
4. McClusky, S., Reilinger, R., Mahmoud, S., Ben Sari, D. & Tealab, A. GPS constraints on Africa (Nubia) and Arabia plate motions. *Geophys. J. Int.* **155,** 126–138 (2003).
5. Chu, D. & Gordon, R. Evidence for motion between Nubia and Somalia along the Southwest Indian Ridge. *Nature* **398,** 64–67 (1998).
6. Maguire, P. *et al.* Geophysical project in Ethiopia studies continental breakup. *Eos* **84,** 337–340 (2003).
7. Ebinger, C. J. & Casey, M. Continental breakup in magmatic provinces: An Ethiopian example. *Geology* **29,** 527–530 (2001).
8. Mackenzie, G. D., Thybo, H. & Maguire, P. K. H. Crustal velocity structure across the Main Ethiopian Rift: results from 2-dimensional wide-angle seismic modelling. *Geophys. J. Int.* (in the press).
9. Bastow, I., Stuart, G. W., Kendall, J-M. & Ebinger, C. J. Upper-mantle seismic structure in a region of incipient continental breakup: Northern Ethiopian Rift. *Geophys. J. Int.* (submitted).
10. Silver, P. G. Seismic anisotropy beneath the continents. *Annu. Rev. Earth Planet. Sci.* **24,** 385–432 (1996).
11. Savage, M. Seismic anisotropy and mantle deformation: What have we learned from shear wave splitting. *Rev. Geophys.* **37,** 65–106 (1999).
12. Gao, S. *et al.* SKS splitting beneath continental rift zones. *J. Geophys. Res.* **102,** 22781–22797 (1997).
13. Ayele, A., Stuart, G. W. & Kendall, J.-M. Insights into rifting from shear-wave splitting and receiver functions: an example from Ethiopia. *Geophys. J. Int.* **157,** 354–362 (2004).
14. Walker, K., Nyblade, A. A., Klemperer, S. L., Bokelmann, G. H. R. & Owens, T. J. On the relationship between extension and anisotropy: Constraints from shear wave splitting across the East Africa Plateau. *J. Geophys. Res.* **109,** doi:10.1029/2003JB002866 (2003).
15. Gashawbeza, E. M., Klemperer, S. L., Nyblade, A. A., Walker, K. T. & Keranen, K. M. Shear-wave splitting in Ethiopia: Percambrian mantle anisotropy locally modified by Neogene rifting. *Geophys. Res. Lett.* **31,** doi:10.1029/2004GL020471 (2004).
16. Hadiouche, O., Jobert, N. & Montagner, J.-P. Anisotropy of the African Continent inferred from surface waves. *Phys. Earth Planet. Inter.* **58,** 61–81 (1989).
17. Rumpker, G. & Ryberg, T. New 'Fresnel zone' estimates for shear-wave splitting observations from finite difference modelling. *Geophys. Res. Lett.* **27,** 2005–2008 (2000).
18. Barruol, G. & Ben-Ismail, W. Upper mantle anisotropy beneath the African IRIS and GEOSCOPE stations. *Geophys. J. Int.* **146,** 549–561 (2001).
19. Wolfenden, E., Ebinger, C., Yirgu, G., Deino, A. & Ayalew, D. Evolution of the northern Main Ethiopian rift: Birth of a triple junction. *Earth Planet. Sci. Lett.* **224,** 213–228 (2004).
20. Abdelselam, M. & Stern, R. Sutures and shear zones in the Arabia-Nubian shield. *J. Afr. Earth Sci.* **23,** 289–310 (1996).
21. Moore, H. & Davidson, A. Rift structure in southern Ethiopia. *Tectonophysics* **46,** 159–173 (1978).
22. Blackman, D. K. *et al.* Teleseismic imaging of subaxial flow at mid-ocean ridges: travel-time effects of anisotropic mineral texture in the mantle. *Geophys. J. Int.* **127,** 415–426 (1996).
23. Vauchez, A., Tommasi, A., Barruol, G. & Maumus, J. Upper mantle deformation and seismic anisotropy in continental rifts. *Phys. Chem. Earth* **25,** 111–117 (2000).
24. Wolfe, C. J. & Solomon, S. C. Shear-wave splitting and implications for mantle flow beneath the MELT region of the East Pacific Rise. *Science* **280,** 1230–1232 (1998).
25. Kendall, J.-M. Teleseismic arrivals at a mid-ocean ridge: effects of mantle melt and anisotropy. *Geophys. Res. Lett.* **21,** 301–304 (1994).
26. Rooney, T. O., Furman, T., Yirgu, G. & Ayalew, D. Structure of the Ethiopian lithosphere: evidence from mantle xenoliths. *Geochim. Cosmochim. Acta* (submitted).
27. Holtzman, B. K. *et al.* Melt segregation and strain partitioning: Implications for seismic anisotropy and mantle flow. *Science* **301,** 1227–1230 (2003).
28. Sleep, N. H. Lateral flow and ponding of starting plume material. *J. Geophys. Res.* **102,** 10001–10012 (1997).
29. Wernicke, B. Low angle normal faults in Basin and Range province: Nappe tectonics in an extending orogen. *Nature* **291,** 645–648 (1981).
30. Bilham, R. *et al.* Secular and tidal strain across the Ethiopian rift. *Geophys. Res. Lett.* **27,** 2789–2984 (1999).

Supplementary Information accompanies the paper on **www.nature.com/nature**.

Acknowledgements We thank the EAGLE working group[6] and especially L. Asfaw and A. Ayele for help with the EAGLE experiment. We thank SEIS-UK for equipment and technical support. We also thank M. Savage, R. Huismans, T. Furman, R. Buck and E. Calais for comments on the manuscipt and A. Parr for help with the data processing. Funding was provided by NERC-UK grants.

Competing interests statement The authors declare that they have no competing financial interests.

Correspondence and requests for materials should be addressed to J.-M.K. (m.kendall@earth.leeds.ac.uk).